Mon. Not. R. Astron. Soc. **376,** 645–650 (2007) doi:10.1111/j.1365-2966.2007.11464.x

Observing cosmic microwave background polarization through ice

Luca Pietranera,[1,2]★ Stefan A. Buehler,[3] Paolo G. Calisse,[2] Claudia Emde,[4] Darren Hayton,[2] Viju Oommen John,[5] Bruno Maffei,[1] Lucio Piccirillo,[1] Giampaolo Pisano,[1] Giorgio Savini[2] and T. R. Sreerekha[6]

[1]*School of Physics and Astronomy, University of Manchester, Manchester M13 9PL*
[2]*School of Physics and Astronomy, Cardiff University, Cardiff CF24 3AA*
[3]*Institut fr Umweltphysik, Universität Bremen, Bremen 28359, Deutschland*
[4]*Deutsches Zentrum fuer Luft- und Raumfahrt (DLR) Institut fuer Physik der Atmosphaere, Oberpfaffenhofen D-82234, Germany*
[5]*Rosenstiel School of Marine and Atmospheric Sciences, University of Miami, USA*
[6]*Met Office, Exeter EX1 3PB*

Accepted 2006 December 27. Received 2006 December 24; in original form 2006 August 16

ABSTRACT

Ice crystal clouds in the upper troposphere can generate polarization signals at the μK level. This signal can seriously affect very sensitive ground-based searches for E and B modes of cosmic microwave background polarization. In this paper, we estimate this effect within the C_ℓOVER experiment observing bands (97, 150 and 220 GHz) for the selected observing site (Llano de Chajnantor, Atacama desert, Chile). The results show that the polarization signal from the clouds can be of the order of or even bigger than the cosmic microwave background expected polarization. Climatological data suggest that this signal is fairly constant over the whole year in Antarctica. On the other hand, the stronger seasonal variability in Atacama allows for a 50 per cent of clean observations during the dry season.

Key words: atmospheric effects – techniques: polarimetric – cosmic microwave background – cosmology: observations.

1 INTRODUCTION

C_ℓOVER (C_ℓObserVER) is a collaboration between the Cardiff Astronomy Instrumentation Group, Oxford Astrophysics, Manchester Astrophysics and the Cavendish Astrophysics Group in Cambridge, on an experiment to measure the cosmic microwave background (CMB) polarization (Maffei et al. 2004).

Polarization of the CMB is caused by Thomson scattering of CMB photons at the last scattering surface (Hu & White 1997). The signal can be decomposed into a curl and a curl-free component known as B and E modes. The B-mode signal, which is at best one order of magnitude weaker than the E mode, is generated by primordial tensor perturbations and therefore its detection would provide valuable information about the history of the early universe.

The main ambitious objective of C_ℓOVER is the measurement of the B mode; in order to achieve this result the experiment will deploy large format imaging arrays, operating at 97, 150 and 220 GHz with 30 per cent bandwidth and a beamwidth of approximately 8 arcmin; the instrument is designed with an unprecedented level of systematic control and will be deployed in the Atacama desert (Chile) at an altitude of 5080 m. Alternative sites are the Antarctic stations of Dome C and South Pole.

★E-mail: luca.pietranera@astro.cf.ac.uk

In spite of a site choice with favourable atmospheric conditions, we expect the signal of the atmospheric fluctuations to be well above the intrinsic instrumental noise.

Since the C_ℓOVER receiver modulates signal polarization, the main concern about atmospheric effects is about a potentially polarized signal from the atmosphere. Water vapour is the major absorbing component at mm wavelengths and its spatial distribution is highly variable with time.

These variations could also introduce some polarization noise; *in situ* measurements of the turbulence suggest that this polarized contribution to system noise is expected to be Gaussian and negligible during most of the observing time, even in Atacama which should be the worst of the three sites, both because of the stronger day–night thermal cycle and the height of the mean boundary layer that can be from 200 to 2000 m (Giovanelli et al. 2001), with respect to 230 m in South Pole and 30 m in Dome C (Agabi et al. 2006) during winter.

In addition to the variable contribution by water vapour, the strong oxygen features at 120 GHz and around 60 GHz dominate the brightness temperature of the atmosphere in C_ℓOVER's spectral region. The presence of the Earth's magnetic field causes a Zeeman splitting of the energy levels of the oxygen, thus resulting in a polarized emission depending on the relative alignment between the line of sight and the magnetic field. This effect is well known for atmospheric measurements (see von Engeln et al. (1998), and references

cited therein). Keating et al. (1998) discussed its impact on CMB measurements. Hanany & Rosenkranz (2003) estimated that the circularly polarized component is not negligible if the intrinsic leakage between linear and circular polarization in the instrument will be of the order of 1 per cent.

However, the polarized intensity due to oxygen is not expected to vary with time but is be fixed for a particular azimuth and elevation direction. Hence any scanning strategy will modulate any residual atmospheric signal in a very predictable way. Also, the estimates are for the DC level of the signal. Oxygen is well mixed in the atmosphere at altitudes up to approximately 80 km, hence fluctuations in the oxygen signal on the angular scales to which C_ℓOVER is sensitive will be very small. It should therefore be possible to separate this signal from the CMB polarization well down below the sensitivity required.

Upper tropospheric ice clouds (like cirrus clouds) represent another source of polarized radiation. These clouds are at high altitudes and contribute to the energy budget of the atmosphere (greenhouse effect) since they absorb thermal infrared radiation from the ground and, as they are cold, emit little infrared radiation. This warms up the Earth-atmosphere system. On the other hand, ice clouds reflect incoming solar short wave radiation and hence cool the Earth-atmosphere system.

At mm and submm wavelengths the interaction between ice clouds and radiation is mainly due to scattering. Absorption is negligible, and so is the thermal emission. The scattering by ice clouds will introduce a polarization signal. Teichmann, Buehler & Emde (2006) have shown that this polarization signal arises even assuming spherical ice particles, due to the asymmetry of the radiation field in the atmosphere. However, real cloud ice particles are not spherical (Wallace & Hobbs 1977), and this increases the polarization signal. Moreover, there is a growing evidence of horizontal alignment of cloud ice particles due to a combination of aerodynamic and gravitational forces (Prigent et al. 2005), which further increases the polarization signal. The actual magnitude of the cloud polarization signal will depend strongly on the particle size and shape, and on the line of sight direction.

Experimentally, ice crystal depolarization is a well-known problem for high frequencies satellite telecommunications (20–50 GHz) based on signal polarization diversity encoding (Martellucci, Poiares Baptista & Blarzino 2002). Measurements carried out with experimental telecommunication payloads (ITALSAT and OLYMPUS) showed that even at relatively low frequencies (with respect to C_ℓOVER bands) the depolarizing effect of ice crystals is not negligible (Trione 2003).

For CMB measurements, the impact of the cloud scattering is twofold. First, the CMB signal is depolarized, similarly to a telecommunication signal. Secondly, the cloud also scatters back upwelling thermal radiation from the earth surface into the line of sight of the instrument. For telecommunication links, this second effect is negligible, due to the large intensity of the telecommunication signal. However, for CMB measurements the radiation scattered back by the atmosphere will often be more intense than the CMB signal. The backscattered signal will be partially polarized, and its polarization characteristics will depend on many factors, as will be explained in the following sections.

2 ICE IN THE UPPER TROPOSPHERE FOR THE THREE SITES

Although ice clouds play an important role in the atmosphere energy budget, up to now they are poorly measured and modelled.

Satellites provide global measurements of integrated ice mass (ice water path – IWP) with frequent revisit time on a long-term basis. Sensors detect both reflected sunlight (in the UV and visible; Buriez et al. 1997) and thermal emission. While the last method is limited to semitransparent clouds the first one only works if the earth surface albedo is not too high (which, unfortunately, is exactly the case for Atacama desert and Antarctica).

The MODIS instrument carried by the Terra and Aqua EOS–NASA satellites is equipped with a cirrus clouds detection band at 1.38 μm; the method, first suggested by Gao, Goetz & Wiscombe (1993) for airborne measurements, suffers the same drawback since it assumes that upwelling radiation reflected by the earth surface is strongly absorbed by water vapour in the lower troposphere and therefore the method is not effective when water vapour column density is very low [i.e. <4 kg m^{-2} corresponding to 4-mm precipitable water vapour (PWV)].

The next generation satellite or airborne instrument will characterize ice clouds by measuring from above the radiation brightness temperature depression with imaging radiometers in the mm and submm range, as proposed by Buehler et al. (2005) and Evans et al. (2002) and will include also polarization measurements (Hayton et al. 2003). *In situ* and aircraft-borne experiments provide the most accurate information on ice clouds. Dual polarization radars (30–90 GHz), polarization diversity lidars and airplanes equipped with cameras are used to characterize ice density, crystal shapes, orientation and size distribution.

As mentioned above, there is evidence that ice needles and plates (especially those with large size and aspect ratio) have a preferred orientation. As crystals drift downwards, they become oriented in a maximum drag condition: aerodynamic forces tend to cause their long axis (or axes) to fall horizontally (i.e. the shortest axis is perpendicular to the ground; see Evans et al. (1998) and references therein for both models and some experimental results). Such a good orientation is testified also by the relatively frequent presence of optical effects, such as sun haloes, which happens only if the crystals are aligned within few degrees. More recently, Noel & Sassen (2005) derived this result from polarized lidar backscatter measurements. Noel & Chepfer (2004) analysed polarized visible light measurements from the POLDER satellite, and found that 50 per cent of high clouds show a glint signature implying at least a fraction of the ice platelets to be horizontally aligned (within a very narrow angle). Davis et al. (2005) showed that cloud ice crystals generate a polarization signal in the limb measurements at 122 GHz [carried out by the Microwave Limb Sounder (MLS) on the Aura satellite]. They also concluded that the effective particle shape can be approximated by a horizontally oriented oblate spheroid with an aspect ratio of 1.3. This rather moderate value of the effective asphericity is due to the fact that, while there are individual particles with large aspect ratios, there is also an averaging effect over the different sizes, shapes and orientations of the individual ice particles.

The purpose of this paper is to estimate the influence of cloud ice particles on the C_ℓOVER measurements at the selected and at the two backup sites (Table 1). For this purpose, assumptions are made on the range of cloud ice amount to be expected for the different sites, as well as on the ice particles size, shape and orientation.

We used the general circulation model of the European Centre for Medium Range Weather Forecasting (ECMWF; see Uppala et al. (2005)) to estimate the statistics of cloud ice mass. Fig. 1 shows the statistics in the form of percentiles. It shows for example that Atacama, though generally a very dry place, can have ice clouds exceeding an IWP (i.e. ice column density, IWP hereafter) of

Table 1. Candidate C$_\ell$OVER observation sites.

Site name	Latitude (°)	Longitude (°)	Height (m)
Atacama	23 S	67 W	5080
Dome C	75 S	123 E	3280
South Pole	90 S	–	2900

100 g m^{-2} for about 10 per cent of the time from December to May. These statistics were derived from a three years long (2000–2002) data set obtained with a gridded version of the ECMWF model data with a grid resolution of 1.5° by 1.5°. A longer data set is still under analysis, however, we believe that the period considered is quite significant since it was not affected by climatic extremes (such as El Nients in South America).

As expected, Atacama shows a much stronger seasonal variability than Antarctica, in the driest season IWP is often (25 per cent of time) $\leqslant$0.0001 g m^{-2}. Since this is the selected site for C$_\ell$OVER experiment, we evaluated the polarized signal from ice crystals using a standard atmospheric profile for these latitudes, rescaled in accordance with locally measured water vapour values (1-mm PWV, i.e. 1 kg m^{-2}).

The impact on CMB polarization measurements will be discussed for a wide range of IWP values from 0.0001 g m^{-2} to 100 g m^{-2}.

3 SCATTERING MODEL

There are no direct data available for particle size, shape and orientation. A realistic size distribution based on the literature was adopted. Ice crystals were assumed to be hexagonal columns, for IWP $<$ 1 g m^{-2} (Ivanova et al. 2001) and compact polycrystals for IWP $\geqslant$ 1 g m^{-2} (Donovan 2003). All particles were horizontally aligned with random azimuthal orientation. The equal-volume-ellipsoid aspect ratio of the particles is assumed to be 1.3.

The radiative transfer (RT) model used for this study is able to handle also even more realistic cases, but for this first assessment it was decided to keep the assumptions as simple as possible for clarity.

The RT model used was the Atmospheric RT Simulator (ARTS). The basics of the model are described by Buehler et al. (2005). Here we used version ARTS-1-1-1095, which can simulate the scattering of radiation by cloud particles (Eriksson et al. 2005). ARTS offers two different scattering algorithms: a Monte Carlo algorithm and an iterative discrete ordinate algorithm (DOIT). In this work we used the DOIT algorithm, which is described in detail by Emde et al. (2004).

The clear-sky part of ARTS has been compared against a range of other microwave RT models (Melsheimer 2005) and against co-located AMSU data and radiosonde profiles (Buehler et al. 2004). The scattering part of ARTS has been compared against several other scattering models (Emde 2005; Hoepfner & Emde 2005), against

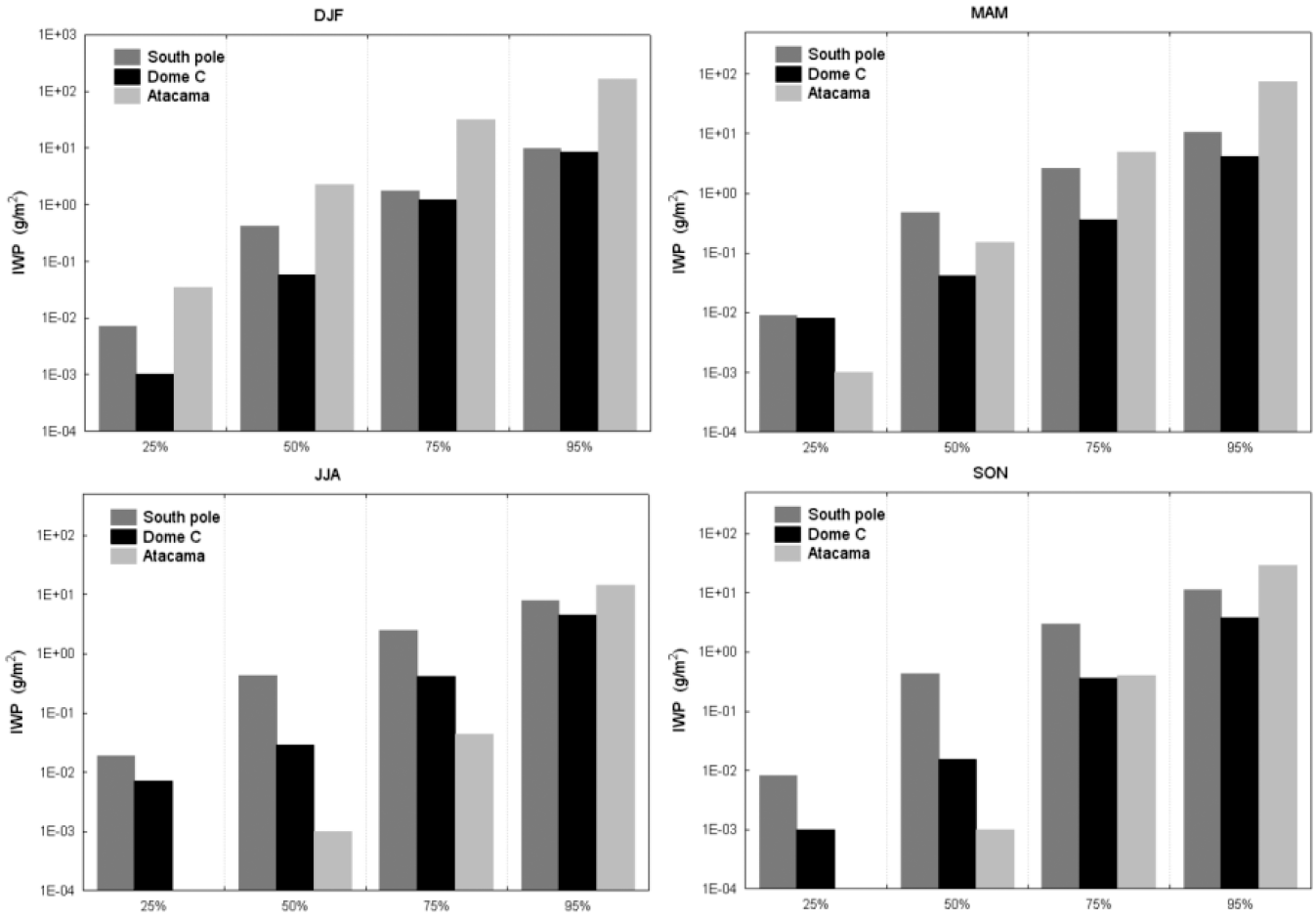

Figure 1. IWP percentiles (values express column density, units are g m^{-2}); each graph represents a three month period. IWP values for the 25 per cent percentile in Atacama, during JJA and SON, are $\leqslant$0.0001 g m^{-2}.

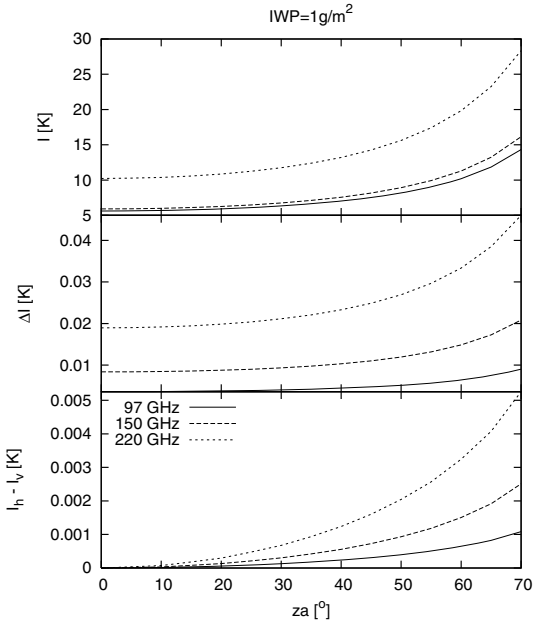

Figure 2. Simulated cloudy radiances, radiance difference and polarization difference between a cloudy and a clear sky as a function of instrument zenith angle. Different curves are for different observation frequencies.

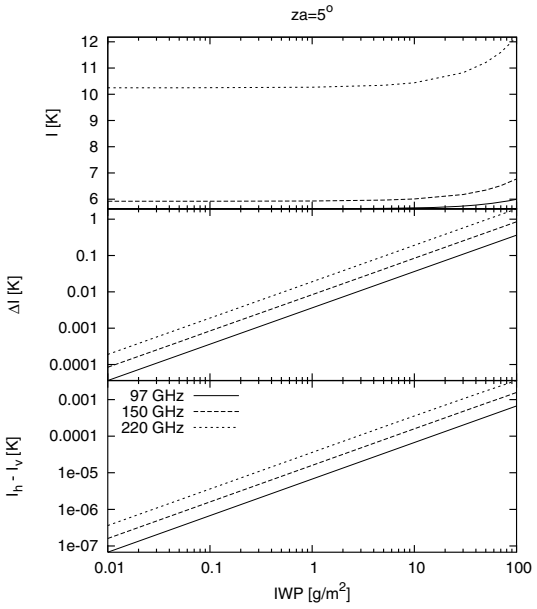

Figure 3. Simulated radiance, radiance difference and polarization difference between a cloudy and a clear sky at a zenith angle of 5° as a function of IWP.

co-located AMSU data and mesoscale weather prediction model fields (Sreerekha et al. 2005).

ARTS can handle all four stokes components. However, the azimuthally symmetric geometry in this case implies that only I and Q stokes components are non-zero. The component I represents the total intensity (sum of horizontally and vertically polarized intensities), the component Q represents the linear polarization difference.

4 RESULTS

Fig. 2 shows the ARTS simulation results. The sensor was assumed to be at an altitude of 5080 m. The cloud was assumed to be located at an altitude of 9000–11 000 m. Each of the plots includes three curves corresponding to the central frequencies of the C$_\ell$OVER bands. The assumed IWP value is IWP $= 1$ g m^{-2}. The different rows show the simulated radiance (top row), the radiance difference (i.e. difference between the radiance from the cloud and the clear sky, middle row) and the polarization difference (Stokes component Q, bottom row). All signals are shown as a function of the instrument angle relative to the zenith direction. The polarization signal is zero at the zenith, and increases with zenith angle.

Both the radiance difference and the polarization signal increase with the IWP. This is shown more clearly in Fig. 3, where the simulated radiance, the radiance difference and the polarization difference are plotted as a function of IWP for a zenith angle of 5°. The figure covers values of IWP ranging from 0.01 to 100 g m^{-2}. Note that the RT is in the linear regime at these frequencies for reasonable IWP values. (Note the logarithmic x-scale of the plots.)

5 EFFECT ON OBSERVED CMB POLARIZATION

The results of the calculations using ARTS show the expected polarization signal induced by the ice clouds. The signal represents the difference between a cloudy and clear sky. Cloud parameters are derived from climatological data.

This signal is divided into two components:

(i) upwelling radiation, emitted by ground and lower atmosphere, that is backscattered and polarized by the ice crystal clouds;

(ii) CMB radiation that is forward-scattered by the ice with a variation in its polarization (ARTS model assumes that CMB radiation is unpolarized).

In order to disentangle the two components, we run the ARTS model alternately imposing $T_{\rm ground}$ and $T_{\rm CMB}$ equal to 0° K. Table 2 shows the polarization signal per unit IWP, which is applicable in the linear regime (at least up to 100 g m^{-2}).

In order to compare the ice crystal induced polarization with the expected cosmological signal, we generated the angular power spectrum of the CMB polarization (both E and B modes) in an ACDM (adiabatic cold dark matter) cosmology scenario with tensor to scalar ratio $r = 0.01$ (using CMBFAST code; see Seljak & Zaldarriaga (1996)).

Fig. 4 reports the expected CMB polarization signal power spectrum in terms of the spherical harmonic coefficient ℓ. The range is limited to spatial scales which are relevant for C$_\ell$OVER experiment: between 10° and 10 arcmin (ℓ ranging from 20 to 1000).

Table 2. Simulated polarization signal (Q) per unit IWP at three different zenith angles. For every angle, the total signal and the polarization induced on 2.7-K CMB are quoted.

Frequency (GHz)	Zenith angle 5°		Zenith angle 25°		Zenith angle} 45°	
	$Q_{\rm total}$ (μK/g m^{-2})	$Q_{\rm CMB}$	$Q_{\rm total}$ (μK/g m^{-2})	$Q_{\rm CMB}$	$Q_{\rm total}$ (μK/g m^{-2})	$Q_{\rm CMB}$
97	7.3	3.1	96	48	330	190
150	18	8.5	240	125	790	370
220	40	20	520	260	1700	850

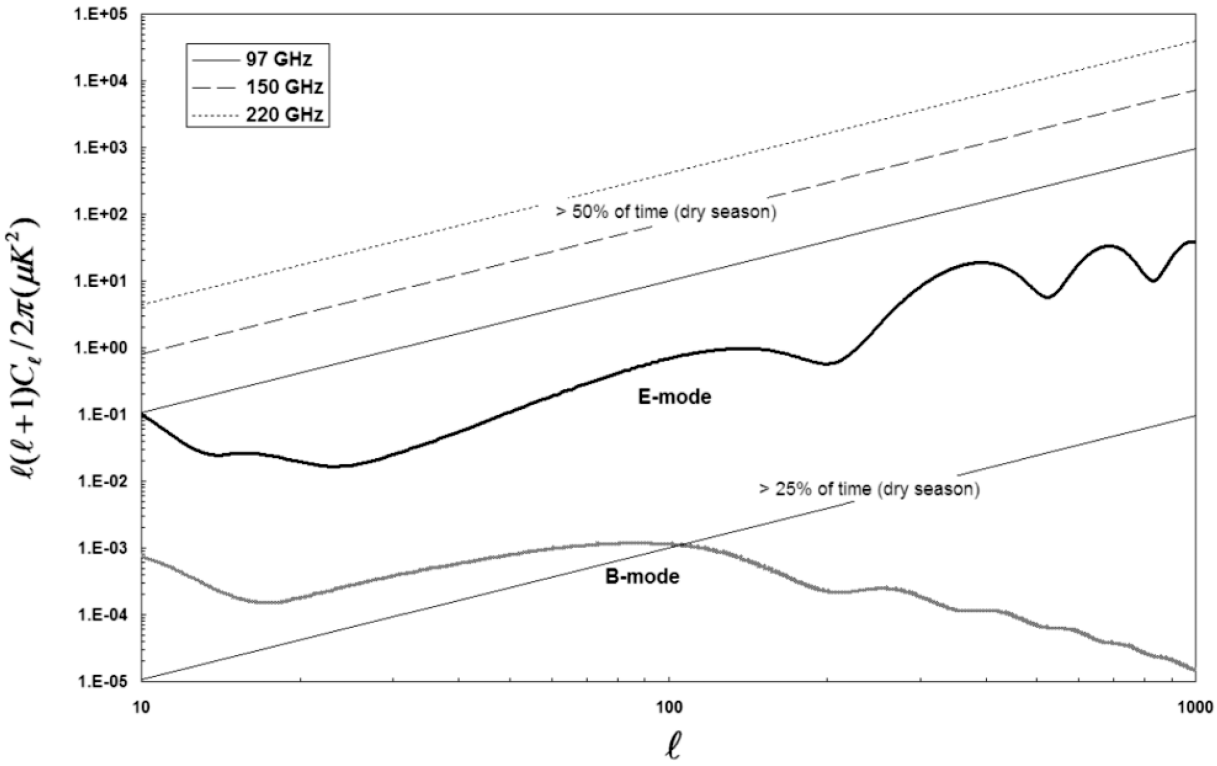

Figure 4. Angular power spectrum of CMB polarization (E and B modes) as calculated by CMBFAST code. Straight lines represent an upper limit on the amount of polarization induced by ice crystal clouds on the 2.7-K CMB for more than 50 per cent observing time during dry season in Atacama (IWP = 0.01 g m^{-2}) at the three C$_\ell$OVER frequencies and an upper limit for 25 per cent observing time during dry season (IWP = 0.0001 g m^{-2}) at 97 GHz. A flat power spectrum is assumed; although it appears that the ice crystal signal might be dominating ground-based observations of CMB polarization of E and B modes, it must be stressed that, while the CMB signal is fixed in the sky, the ice signal is most probably variable with time. Therefore, it is always possible to disentangle and therefore greatly reduce the ice signal from the sky signal by a properly designed observing strategy

The polarization signal on CMB radiation due to ice crystals is plotted for each C$_\ell$OVER frequency, assuming an observing zenith angle of 5° and IWP values corresponding to an upper limit for respectively 50 and 25 per cent of observing time during dry season.

In the figure we arbitrarily assumed a flat power spectrum for the observed signal from ice crystal clouds; it has to be underlined that this model is really inadequate and a more realistic representation should take into account the cirrus cloud morphology and spatial distribution which unfortunately are very poorly known. Qualitatively, a decrease at the high ℓ is expected, since the clouds are supposed to be quite homogeneous at these angular scales, but, in any case, the signal could still be orders of magnitude stronger that the expected B-mode component during a significant fraction of the observing time.

6 CONCLUSIONS

The polarization signal on CMB radiation due to ice crystal clouds cannot be neglected by a ground-based experiment looking for mapping E- and B-mode patterns even for low ice water column density values (0.001 g m^{-2}). The effect is particularly strong for the high frequencies commonly used for CMB measurements (150 GHz and above).

Possible mitigation strategies include the followings.

(i) Constant elevation fast instrument scanning: at the moment C$_\ell$OVER is designed to internally modulate the CMB polarization signal and therefore an absolute measurement of this parameter (i.e. for each pixel) would be possible. A differential approach, based on rapidly measurement of signal differences between contiguous pixels would cancel the constant bias due to ice crystals clouds. However, the measurement would still be affected by the cloud spatial distribution and inhomogeneities.

(ii) IWP could be measured by processing Earth Observing (EO) satellite data. In principle, geostationary satellites near real-time monitoring capabilities (one measurement every 15–30 min). However, as discussed above (Para 2), very low tropospheric water vapour content (both in Atacama and in Antarctica) seriously undermine this measurement. Future EO mission dedicated to ice cloud measurements will be helpful for solving this problem.

(iii) IWP *in situ* measurements can be carried out in order to assess the quality of measured polarization, and to characterize, during clean nights, a set of reference pixels to be used for ice detection. Among the possible options, the use of a polarized lidar, though difficult to deploy and operate, would provide us with a full characterization of ice crystals (shape, size distribution and orientation) allowing an accurate modelling of radiative effects in the microwaves.

In this difficult observational context, a preliminary comparison between the sites can be attempted. The presence of the sun at high elevation angles penalizes Atacama with respect to Antarctica sites; however, due to the high sensitivities required for CMB polarization measurements, it is in any case difficult to carry out measurements with the sun above the horizon (strong signal in the instrument sidelobes). On the other hand climatological data on ice cloud

occurrence and density suggest that Atacama observing conditions during dry seasons are significantly better than Antarctica (with frequent occurrences of IWP $\leqslant 0.0001$ g m^{-2})

ACKNOWLEDGMENTS

Thanks to the ARTS radiative transfer community, many of whom have indirectly contributed by implementing features to the ARTS model.

REFERENCES

Agabi A., Aristidi E., Azouit M., Fossat E., Martin F., Sadibekova T., Vernin J., Ziad A., 2006, PASP, 118, 344

Buehler S. A., Kuvatov M., John V. O., Leiterer U., Dier H., 2004, J. Geophys. Res., 109, D13103

Buehler S. A., Eriksson P., Kuhn T., von Engeln A., Verdes C., 2005, J. Quant. Spectrosc. Radiat. Transfer, 91, 65 (the ARTS model is publicly available at the website http://www.sat.uni-bremen.de/arts/)

Buriez J. C. et al., 1997, Int. J. Remote Sens., 18, 2785

Davis C. P., Wu D. L., Emde C., Jiang J. H., Cofield R. E., Harwood R. S., 2005, Geophys. Res. Lett., 32, L14806

Donovan D. P., 2003, J. Geophys. Res., 108, 4573

Emde C., 2005, PhD thesis, Univ. Bremen

Emde C., Buehler S. A., Davis C., Eriksson P., Sreerekha T. R., Teichmann C., 2004, J. Geophys. Res., 109, D24207

Eriksson P., Buehler S. A., Emde C., Sreerekha T. R., Melsheimer C., Lemke O., 2005, ARTS-1-1 User Guide. University of Bremen, Germany, p. 308 (regularly updated versions available at www.sat.uni-bremen.de/arts/)

Evans K. F., Walter S. J., Heymsfield A. J., Deeter M. N., 1998, J. Appl. Meteorol., 37, 184

Evans K. F., Walter S. J., Heymsfield A. J., McFarquhar G. M., 2002, J. Geophys. Res., 107, 10

Gao B. C., Goetz A. F. H., Wiscombe W. J., 1993, Geophys. Res. Lett., 20, 301

Giovanelli R. et al., 2001, PASP, 113, 789

Hanany S., Rosenkranz P., 2003, New. Astron. Rev., 47, 1159

Hayton D. J., Ade P., Lee C., Evans F., 2003, Proc. SPIE, 5235 586

Hoepfner M., Emde C., 2005, J. Quant. Spectrosc. Radiat. Transfer, 91, 275

Hu W., White M., 1997, New. Astron. 2, 323 (http://astro.berkeley.edu/∼mwhite/polar/)

Ivanova D. C., Mitchell D. L., Patrick Arnott W., Poellot M., 2001, Atmos. Res., 59–60, 89

Keating B., Timbie P., Polnarev A., Steinberger J., 1998, ApJ, 495, 580

Maffei B. et al., 2004, EAS Publication Ser., 14, 251

Martellucci A., Poiares Baptista J. P. V., Blarzino G., 2002, 1st Int. Workshop, COST Action 280, Propagation Impairment Mitigation for Millimetre Wave Radio Systems. Technical Note PM3037

Melsheimer C. et al., 2005, Radio Sci., 40, R1007

Noel V., Chepfer H., 2004, J. Atmos. Sci., 61, 2073

Noel V., Sassen K., 2005, J. Appl. Meteorol., 44, 653

Prigent C., Defer E., Pardo J. R., Pearl C., William B., Rossow W. B., Pinty J. P., 2005, Geophys. Res. Lett., 32, L04810

Seljak U., Zaldarriaga M., 1996, ApJ, 469, 437

Sreerekha T. R., Buehler S. A., English S. J., O'Keeffe U., Doherty A., Emde C. 2005, Q. J. R. Meteorol. Soc., submitted

Teichmann C., Buehler S. A., Emde C., 2006, J. Quant. Spectrosc. Radiat. Transfer, 101, 179

Trione G., 2003, PhD thesis, Politecnico di Milano

Uppala S. M. et al., 2005, Q. J. R. Meteorol. Soc., 131, 2961

von Engeln A., Buehler S. A., Langen J., Wehr T., Kuenzi K., 1998 J. Geophys. Res., 103, 31735

Wallace J. M., Hobbs P. V., 1977, Atmospheric Science. Academic Press, New York

This paper has been typeset from a TEX/LATEX file prepared by the author.